



# Translation Elongation Factor EF-Tu Modulates Filament Formation of Actin-Like MreB Protein *In Vitro*

Hervé Joël Defeu Soufo<sup>1,4</sup>, Christian Reimold<sup>2</sup>, Hannes Breddermann<sup>2</sup>, Hans G. Mannherz<sup>3</sup> and Peter L. Graumann<sup>2</sup>

**1** - Microbiology, Faculty of Biology, University of Freiburg, Schänzlestrasse 1, 79104 Freiburg, Germany

**2** - LOEWE Center for Synthetic Microbiology (SYNMIKRO) and Department of Chemistry, Philipps Universität, 35037 Marburg, Germany

**3** - Abteilung für Anatomie und Molekulare Embryologie, Ruhr-Universität, 44801 Bochum, Germany

**Correspondence to Hervé Joël Defeu Soufo and Peter L. Graumann:** [joel.defeusoufo@biologie.uni-freiburg.de](mailto:joel.defeusoufo@biologie.uni-freiburg.de);

[peter.graumann@synmikro.uni-marburg.de](mailto:peter.graumann@synmikro.uni-marburg.de)

<http://dx.doi.org/10.1016/j.jmb.2015.01.025>

Edited by J. Sellers

## Abstract

EF-Tu has been shown to interact with actin-like protein MreB and to affect its localization in *Escherichia coli* and in *Bacillus subtilis* cells. We have purified YFP-MreB in an active form, which forms filaments on glass slides *in vitro* and was active in dynamic light-scattering assays, polymerizing in milliseconds after addition of magnesium. Purified EF-Tu enhanced the amount of MreB filaments, as seen by sedimentation assays, the speed of filament formation and the length of MreB filaments *in vitro*. EF-Tu had the strongest impact on MreB filaments in a 1:1 ratio, and EF-Tu co-sedimented with MreB filaments, revealing a stoichiometric interaction between both proteins. This was supported by cross-linking assays where 1:1 species were well detectable. When expressed in *E. coli* cells, *B. subtilis* MreB formed filaments and induced the formation of co-localizing *B. subtilis* EF-Tu structures, indicating that MreB can direct the positioning of EF-Tu structures in a heterologous cell system. Fluorescence recovery after photobleaching analysis showed that MreB filaments have a higher turnover in *B. subtilis* cells than in *E. coli* cells, indicating different filament kinetics in homologous or heterologous cell systems. The data show that MreB can direct the localization of EF-Tu *in vivo*, which in turn positively affects the formation and dynamics of MreB filaments. Thus, EF-Tu is a modulator of the activity of a bacterial actin-like protein.

© 2015 The Authors. Published by Elsevier Ltd. This is an open access article under the CC BY-NC-ND license (<http://creativecommons.org/licenses/by-nc-nd/4.0/>).

## Introduction

The shape of the cell usually plays a key role in its physiology and survival. For example, directed motility is mostly described for a rod-shaped or spiral-shaped cell, but not for round bacteria (cocci), except for some round Cyanobacteria [1,2]. Even more importantly, the maintenance of rod-shaped morphology is apparently essential for all bacterial cells analyzed so far because loss-of-function mutations in genes that are involved in cell shape maintenance are lethal or leave the cells barely viable [3,4]. Besides several membrane proteins that are (or are thought to be) involved in the synthesis of the shape-determining cell wall, a central player in the generation of rod or complex cell shape is MreB, the bacterial ortholog of actin. As seen from their structure and the way they form double-filament structures,

MreB and actin clearly share the same ancestor [5]. In addition to ATP, MreB can also employ GTP for the formation of filaments [6], but it forms straight or double-helical filaments, dependent on purification conditions [5,7], rather than just purely helical filaments such as actin [8]. The depletion of MreB in model bacteria such as *Escherichia coli*, *Caulobacter crescentus* or *Bacillus subtilis* results in the generation of round cells, while the cell cycle continues, until cells eventually lyse [9–11]. In contrast, *Helicobacter pylori* cells keep their helical shape but grow very slowly [12]. In all bacteria investigated so far, MreB forms filamentous structures underneath the cell membrane [9,10,11], which interact with membrane proteins MreC and MreD [13–15] and with cell-wall-synthesizing enzymes (e.g., Pbp1) [16], whose loss also affects cell morphology. Interestingly, it has recently been

shown that MreB has an inherent affinity to the cell membrane [17,18] and thus does not need a membrane anchor for proper localization. It has been postulated that the localization of MreB affects the localization of MreC (which also interacts with several Pbps [19]), MreD and of Pbp1, thereby directing the organization of cell wall synthesis, which also occurs in a helical pattern [20]. However, this model has not been stringently proven. It is also still unclear how MreB obtains its localization pattern underneath the cell membrane and what determines the turnover of MreB filaments, which is high in *B. subtilis* and *C. crescentus* cells [21,22] but is apparently low in *E. coli* cells.

We have shown that translation elongation factor EF-Tu forms a structure underneath the cell membrane in *B. subtilis* cells and co-localizes and interacts with MreB [23]. Depletion of EF-Tu affects the localization and dynamics of MreB filaments, which become disorganized and lose their fast remodeling kinetics. Conversely, in *mreB* mutant cells (which can be generated in a special medium), EF-Tu no longer localizes to the helical structures, suggesting that both proteins affect each other's localization. Recently, it has been shown that EF-Tu also interacts with MreB in *E. coli*. With the use of super-resolution microscopy, it was shown that only a subset of EF-Tu and MreB molecules interact, mostly at places close to the cell membrane [24]. EF-Tu has long been proposed to serve an additional role as a cytoskeletal element in many bacteria [25] and, apparently, an interaction with MreB proteins conserved in several bacteria.

We wished to gain further insight into the interplay of EF-Tu and MreB. However, EF-Tu is essential for translation; thus, it is difficult to analyze its direct effect on MreB in *B. subtilis* cells. Therefore, we turned to a

heterologous cell system, expressing *B. subtilis* MreB and EF-Tu in *E. coli* cells, as well as *in vitro* experiments using purified proteins. Our experiments show that EF-Tu stimulates and stabilizes the formation of MreB filaments *in vitro*, and therefore, it is a potential modulator of MreB activity in bacteria.

## Results

### MreB and EF-Tu can be efficiently cross-linked *in vitro*

We used a cross-linking assay to further confirm the physical interaction between MreB and EF-Tu *in vitro*. When expressed, together in *E. coli* cells, Strep-MreB and EF-Tu-His co-purified from the Streptavidin column in an approximately 1:1 ratio, confirming their interaction *in vitro*. The additional band at 70 kDa was determined to be DnaK, the bacterial Hsp70 molecular chaperone, via mass spectrometry (Fig. 1a, lane 1). DnaK is a frequent contamination during heterologous protein expression in *E. coli* [26]. The treatment of the co-purified proteins with the bifunctional cross-linking agent glutaraldehyde resulted in the appearance of new bands on the SDS-PAGE gel. Varying the reaction incubation time over a 15-min period at room temperature did not show any significant difference in banding patterns or intensities (Fig. 1a, lanes 3–5). The bands were gel-excised and their protein constituents were identified by mass spectrometry. Additionally, the bands were blotted onto nitrocellulose membrane and probed with antibodies specific for MreB. The glutaraldehyde cross-linking reaction yielded four additional distinct bands visible on

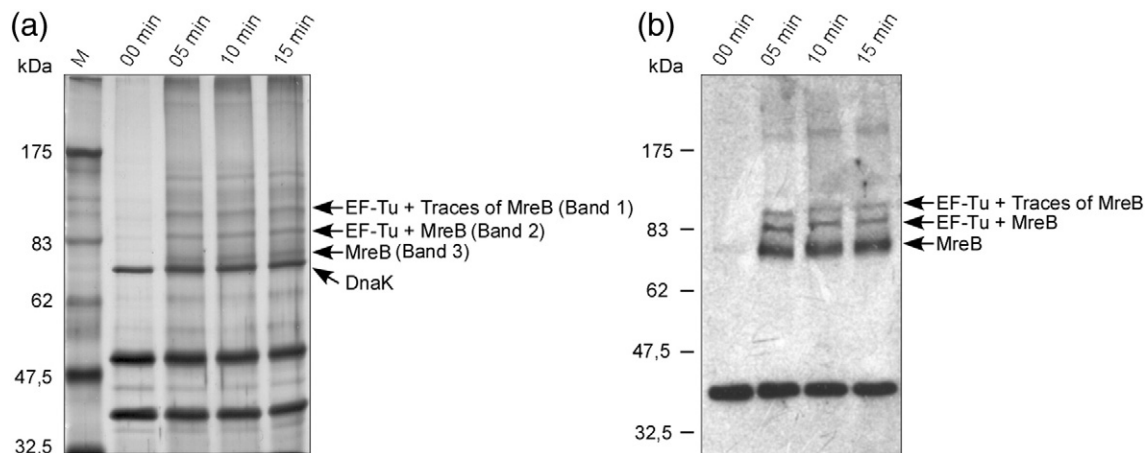


**Fig. 1.** Chemical cross-linking analysis of Strep-MreB and EF-Tu-His by glutaraldehyde. (a) The different cross-linked species were resolved by 8% SDS-PAGE. The constituents of the analyzed bands are indicated. Note that EF-Tu-His ran higher than its expected size of 43.5 kDa. (b) The bands from a gel duplicate in (a) were transferred to nitrocellulose and subjected to Western blotting with anti-MreB antibodies revealing MreB-containing bands. The incubation time of the cross-linking reaction is indicated on each lane.

**Table 1.** Protein components of the analyzed bands as deduced from mass spectrometry data

	Band 1	Band 2	Band 3
Molecular mass (kDa)	125	85	72
Corresponding components	1 × MreB + 2 × EF-Tu	1 × MreB + 1 × EF-Tu	2 × MreB

The sizes of the bands were calculated according to the molecular mass of 35.78 kDa and 43.43 kDa for MreB and EF-Tu, respectively.

silver-stained SDS-PAGE gel (Fig. 1a, lanes 3–5). Three of the four bands were identified as follows: band 1, EF-Tu (corresponding to a size of 2 molecules of EF-Tu and 1 molecule of MreB); band 2, MreB and EF-Tu (corresponding to a size of 1 molecule of MreB and 1 molecule of EF-Tu); and band 3, MreB (corresponding to a size of 2 molecules) (Table 1). Western blot analysis corroborated with the mass spectrometry data. In the absence of glutaraldehyde, anti-MreB recognized a single band of the size of MreB but also stained all MreB-containing bands in the cross-linked samples (Fig. 1b). Importantly, mass spectrometry analysis revealed the same amount of peptides from MreB and EF-Tu in band 2, suggesting 1:1 interaction between the proteins. We also used a second cross-linking reagent, BS3 [bis(sulfosuccinimidyl)suberate], that reacts selectively with lysine amino groups and obtained the same banding pattern as with glutaraldehyde (Supplementary Fig. 1). These data indicate that MreB and EF-Tu can exist as homodimers in solution and suggest that EF-Tu and MreB interact in a 1:1 stoichiometry.

### EF-Tu positively affects the formation of MreB filaments *in vitro*

To investigate the effect of EF-Tu on MreB polymerization, we turned to a system employing purified proteins. MreB, YFP-MreB and EF-Tu could be purified as soluble proteins using Strep affinity tags. All proteins were purified to an apparent purity of >95% and stored in the polymerization buffer containing ATP (Fig. 2a). When YFP-MreB (or MreB) was subjected to ultracentrifugation, >95% of the protein remained in the supernatant (Fig. 2b, lanes 2 and 3; Supplementary Fig. 2, lanes 1 and 2 and lanes 5 and 6). In contrast, the addition of MgCl<sub>2</sub> followed by 15 min of incubation induced the formation of MreB filaments that sedimented upon centrifugation (Fig. 2b, lanes 4 and 5; Supplementary Fig. 2, lanes 3 and 4 and lanes 7 and 8). Addition of EF-Tu to this reaction in a 0.5:2 molar ratio relative to MreB resulted in an increased sedimentation of MreB (Fig. 2b, compare lanes 4 and 5 with lanes 11 and 12; note the decrease in intensity of the soluble fraction). When *E. coli* cell extract lacking EF-Tu was

loaded onto a Streptavidin column, elution fractions did not have an influence on the polymerization of MreB as judged from the amount found in the pellet fraction (Supplementary Fig. 2, lanes 21 and 22). Addition of EF-Tu in a 1:1, 2:1 and 4:1 molar ratio to MreB further increased the amount of MreB in the pellet (Fig. 2b, lanes 13–18; Supplementary Fig. 2, lanes 15–20). EF-Tu alone, that is, in the absence of MgCl<sub>2</sub>, did not induce the formation of MreB filaments (Supplementary Fig. 2, lanes 13 and 14). EF-Tu also appeared in the pellet fraction by itself upon addition of MgCl<sub>2</sub> (Fig. 2b, lanes 6–10). However, when incubated together with MreB, more EF-Tu was found in the pellet fraction than for EF-Tu by itself (Fig. 2b, compare lanes 9 and 10 with lanes 13 and 14), indicating that a considerable amount of EF-Tu was bound to MreB filaments or induced to sediment through the interaction with MreB.

To verify these *in vitro* findings, we performed fluorescence microscopy analyses, where purified YFP-MreB was induced to form filaments on glass slides, which is compatible with MreB polymerization. YFP-MreB built up structures ranging from punctuated spots to up to several micrometer-long filaments under fluorescence microscope conditions, 10 min after the addition of MgCl<sub>2</sub> [Fig. 3b–d; Supplementary Fig. 3a(b)–a(d)] but not in the absence of MgCl<sub>2</sub> [Fig. 3a; Supplementary Fig. 3a(a)]. Note that many filaments did not stick to the glass surface along their entire length but extended away from the surface. Many filaments appeared to be branched, curved or helical. These findings suggest that MreB filaments are composed of bundles of protofilaments, which are quite flexible in terms of their architecture. It was not possible to follow the time-resolved extension of YFP-MreB filaments under the microscope. Apparently, filaments formed rather spontaneously and extended quickly to their average size, such that intermediates were difficult to catch. This is consistent with the highly rapid polymerization of MreB observed in light-scattering experiments described below. However, when EF-Tu was added to YFP-MreB, the number of filaments and their length strongly increased [Fig. 3e and f; Supplementary Fig. 3b(a)–b(c)] to reach a maximum length of ~35 μm (Fig. 4a). Note that YFP-MreB alone at an equivalent molar concentration of YFP-MreB plus EF-Tu did not polymerize to the same extent as both proteins together [compare Supplementary Fig. 3c with Supplementary Fig. 3b(c)]. The quantification of the fluorescence intensity of polymerized YFP-MreB was determined using ImageJ. For accurate measurements, the uneven background in the images was first subtracted using the “Subtract Background” tool. The measurements of the integrated fluorescence density of the total area and the three-dimensional graphs of the intensities of image pixels verified that EF-Tu enhanced the assembly of MreB polymer in a

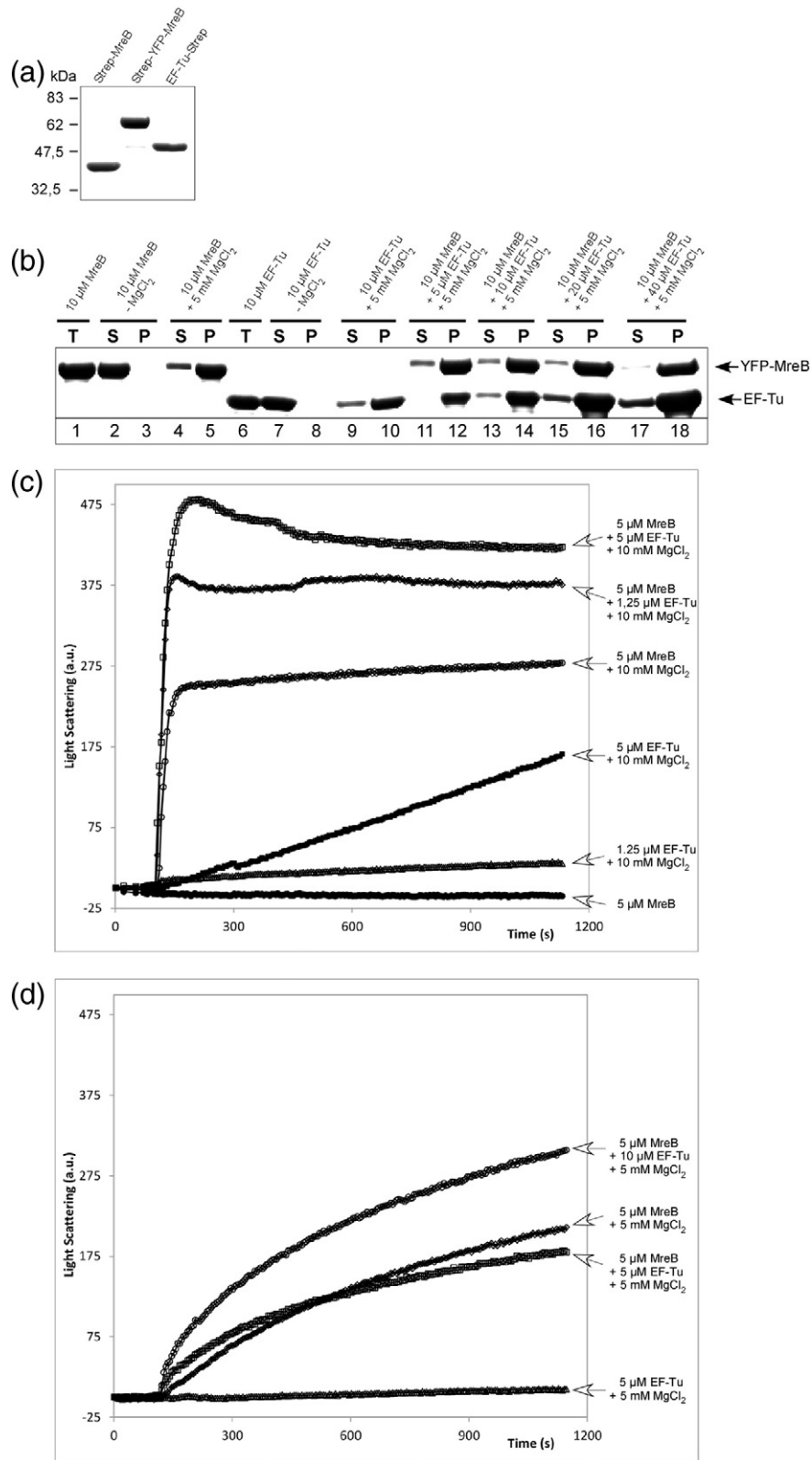


Fig. 2 (legend on next page)

dose-dependent manner (Fig. 4b and c). These experiments further support the finding that EF-Tu positively affects filament formation of MreB *in vitro*.

### EF-Tu enhances the rate of formation of MreB filaments

We wished to obtain information on the effect of EF-Tu on the dynamics of filament formation of MreB filaments and to address the question if EF-Tu acts upon preassembled MreB filaments or during filament assembly. For this purpose, light scattering was employed. Purified YFP-MreB (or MreB) induced pronounced light scattering upon the addition of magnesium to the system (ATP was present in the buffer) (Fig. 2c), as described before [6]. Interestingly, filament formation occurred without a lag phase within few seconds, rather than in minutes as described for actin filaments [27,28], revealing that MreB has the ability to polymerize much more rapidly than actin. Upon addition of magnesium (10 mM MgCl<sub>2</sub>), EF-Tu showed a slow and marginal increase in scattering compared with MreB (Fig. 2c). These experiments show that EF-Tu does not form fast-growing polymer structures under our experimental conditions. Addition of elution fractions from *E. coli* lacking EF-Tu did not affect filament dynamics of MreB or of YFP-MreB (data not shown). However, the addition of EF-Tu to MreB in a 1:4 ratio led to a more than 1.5-fold increment of the slope of scattered light (Fig. 2c), showing that EF-Tu enhances the rate of MreB filament assembly. Adding more EF-Tu to the reaction mixture (i.e., a 1:1 ratio relative to MreB) induced more scattering but did not further increase the speed of MreB polymerization (Fig. 2c). At a lower concentration of magnesium (5 mM MgCl<sub>2</sub>), where polymer formation is slower, the effect of EF-Tu on MreB polymerization was even more pronounced and resulted in a 2-fold or 3.5-fold increase in the speed of MreB polymerization, in 1:1 or 2:1 molar ratio relative to the concentration of MreB, respectively (Fig. 2d). Thus, at a 1:1 molar or even lower stoichiometry, EF-Tu markedly affects the rate and amount of polymer formation of MreB, in agreement with the fluorescence microscopy analysis.

### *B. subtilis* MreB directs the localization of *B. subtilis* EF-Tu in a heterologous cell system

MreB and EF-Tu affect each other's localization in *B. subtilis* cells [23] and also interact with each other in *E. coli* cells [24]. On the other hand, when heterologously expressed in *E. coli*, *B. subtilis* MreB does not co-localize with *E. coli* MreB but forms distinct filamentous structures [29]. We asked the question if *B. subtilis* MreB can associate with *B. subtilis* EF-Tu in a heterologous cell system. Expression levels in *E. coli* cells were chosen such that a similar level of MreB compared with *B. subtilis* cells was achieved using Western blotting [29]. Although YFP-MreB filaments appeared to have a typical arrangement described for *B. subtilis* in a large fraction of the cells (about 30%), most cells contained rather irregularly positioned filaments, which can frequently be followed to extend through the entire cell. *E. coli* cells still grew and extended upon induction of YFP-MreB and eventually obtained a larger size (Figs. 5b and 6b), as observed before [29]. In contrast to YFP-MreB, EF-Tu-CFP did not form any filaments when expressed in *E. coli* cells and did not induce any cell shape deformation, indicating that *B. subtilis* EF-Tu does not perturb the function of *E. coli* MreB or of any other morphogenic protein. Rather, it was heterogeneously distributed throughout the cells (Fig. 5a) or accumulated at polar zones surrounding the nucleoids in a subpopulation of the cells (Supplementary Fig. 4), where the bulk of the ribosomes are present [30–32]. These findings indicate that *B. subtilis* EF-Tu may function in translation in *E. coli* cells but does not form filamentous structures by itself. However, when EF-Tu-CFP and YFP-MreB were co-expressed, defined filamentous EF-Tu-CFP structures were observed in about 35% of cells, which invariably co-localized with YFP-MreB filaments (Fig. 5c, with 200 cells analyzed). Thus, *B. subtilis* MreB can recruit *B. subtilis* EF-Tu to the filamentous structures *in vivo* in a heterologous cell system, in agreement with the findings from *B. subtilis* [23]. The expression level of EF-Tu varied considerably between individual cells, as well as the number of YFP-MreB filaments. Therefore, it was difficult to determine if the

**Fig. 2.** Effect of EF-Tu on MreB filaments *in vitro*. (a) Coomassie-stained 12% SDS-PAGE of purified Strep-MreB, Strep-YFP-MreB and EF-Tu-Strep. (b) Coomassie-stained SDS-PAGE of sedimentation assays; S, supernatant; P, pellet; lane 1, total YFP-MreB used in the centrifugations; lanes 2 and 3, YFP-MreB after centrifugation; lanes 4 and 5, YFP-MreB plus ATP and MgCl<sub>2</sub> after centrifugation; lane 6, total EF-Tu added in lanes 7–10; lanes 11–18, YFP-MreB plus ATP plus MgCl<sub>2</sub> plus purified EF-Tu (added in 1:0.5, 1:1, 1:2 and 1:4 molar ratios to MreB). (c) Plot of light-scattering intensity of MreB assembly as a function of time (s) in the presence or absence of EF-Tu: MreB plus ATP (filled circles), EF-Tu plus ATP plus MgCl<sub>2</sub> (open triangles), MreB plus ATP plus MgCl<sub>2</sub> (open circles), MreB plus ATP plus EF-Tu (1:0.25 molar ratio to MreB) plus MgCl<sub>2</sub> (open diamonds) and MreB plus ATP plus EF-Tu (1:1 molar ratio to MreB) plus MgCl<sub>2</sub> (open squares). We added 10 mM MgCl<sub>2</sub> at minute 2 to start the formation of MreB filaments. (d) Similar experiment as described in (c), in the presence of a lower concentration of MgCl<sub>2</sub> (5 mM): EF-Tu plus ATP plus MgCl<sub>2</sub> (open triangles), MreB plus ATP plus MgCl<sub>2</sub> (open diamonds), MreB plus ATP plus EF-Tu (1:1 molar ratio to MreB) plus MgCl<sub>2</sub> (open squares) and MreB plus ATP plus EF-Tu (1:2 molar ratio to MreB) plus MgCl<sub>2</sub> (open circles). We added 5 mM MgCl<sub>2</sub> at minute 2 to start the formation of MreB filaments.

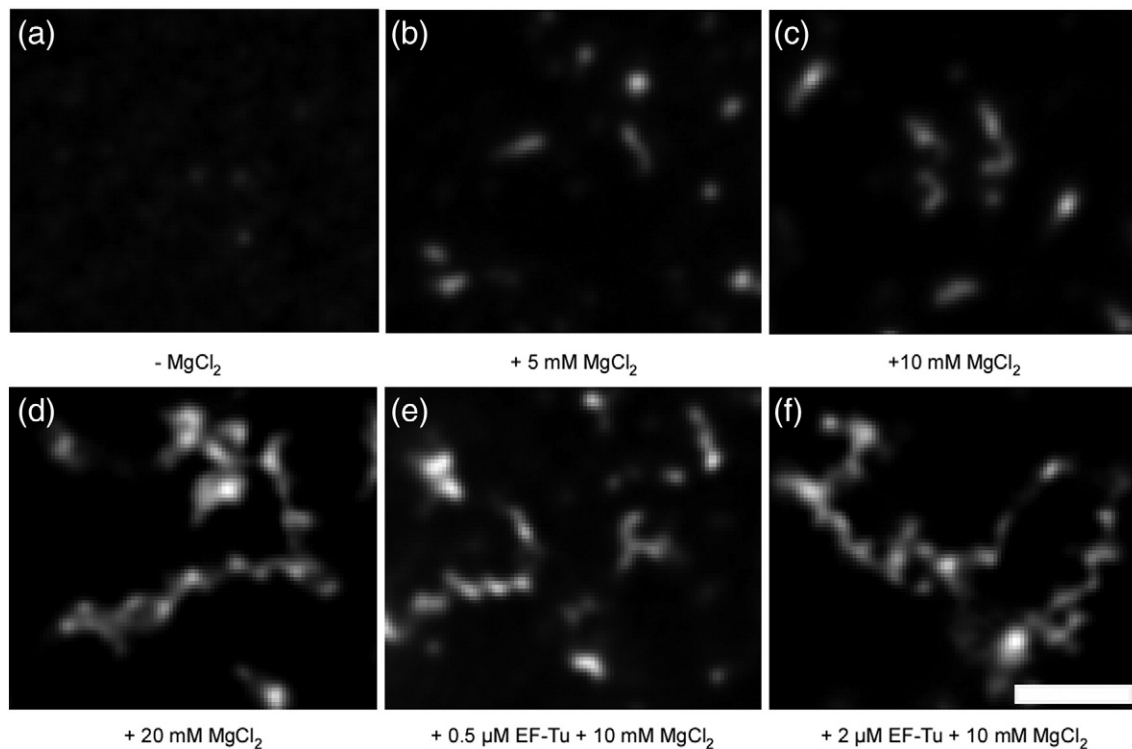


**Fig. 3.** Fluorescence micrographs of purified YFP-MreB *in vitro* on glass slides after 10 min of incubation at 25 °C. (a) Shown is 2  $\mu$ M YFP-MreB in the presence of ATP only. (b–d) Shown is 2  $\mu$ M YFP-MreB in the presence of ATP and different concentration of  $MgCl_2$ : 5 mM (b), 10 mM (c) and 20 mM (d). (e and f) Shown is the effect of EF-Tu on YFP-MreB filaments formation in the presence of ATP and  $MgCl_2$ : 2  $\mu$ M YFP-MreB plus 0.5  $\mu$ M EF-Tu (e) and 2  $\mu$ M YFP-MreB plus 2  $\mu$ M EF-Tu (f). Scale bars represent 2  $\mu$ m.

induction of EF-Tu had an effect on the amount or on dynamics of MreB filaments.

### MreB filaments in *B. subtilis* cells have a different turnover than those formed heterologously in *E. coli* cells

We wished to investigate if the dynamics of MreB filaments change when they are expressed in different cell systems. We therefore performed time lapse and fluorescence recovery after photobleaching (FRAP) experiments, which reveal the dynamics and exchange of FP-labeled subunits of filaments with unbound subunits, in *B. subtilis* cells (we bleached an area as small as possible instead of a whole cell half; Fig. 6a) and in a heterologous cell system, using expression in *E. coli* cells (Fig. 6b). It is important to note that N-terminally FP-labeled protein was shown to be expressed at wild-type level and was functional in that it complemented efficiently the *mreB* deletion or depletion mutant in *B. subtilis* [15]. The expression level of YFP-MreB in *E. coli* was set to be similar to *B. subtilis* as determined by Western blotting [29]. When expressed at moderate levels (0.01 mM IPTG), YFP-MreB formed clearly visible filamentous structures in *E. coli* cells (Figs. 5b and 6b). A part of an

MreB filament was bleached and recovery was followed with 200 ms of stream acquisitions (Fig. 6a and b). Figure 6a and c shows that the turnover of MreB filaments in *B. subtilis* is in the range of seconds and, thus, much faster than what was previously reported for MreB and Mbl (2.5–5 min), where cell halves rather than parts of filaments were bleached [15,33]. Half-time recovery of YFP-MreB filaments was 18 s (Fig. 6c), compared with a half-time of 0.3 s for a freely diffusing protein of similar size [34] and compared with 9–32 s for the FtsZ ring [35,36]. It is important to point out that MreB filament movement from non-bleached to bleached areas will contribute to rapid protein turnover. During the time window of YFP-MreB recovery, the distance traveled by MreB filaments (25–75 nm/s) will be substantial. In contrast, half-time recovery for YFP-MreB expressed in *E. coli* cells was  $50 \pm 5.3$  s (Fig. 6c). In order to investigate if movement of filaments contributes to FRAP recovery in *E. coli* cells, we performed structured illumination microscopy (SIM) time lapse experiments, which revealed that *B. subtilis* MreB filaments are largely static in *E. coli* cells (Supplementary Movies 1 and 2). Therefore, half-time recovery of 50 s represents the true subunit exchange dynamics of MreB, when it is expressed in a heterologous cell system. Note that

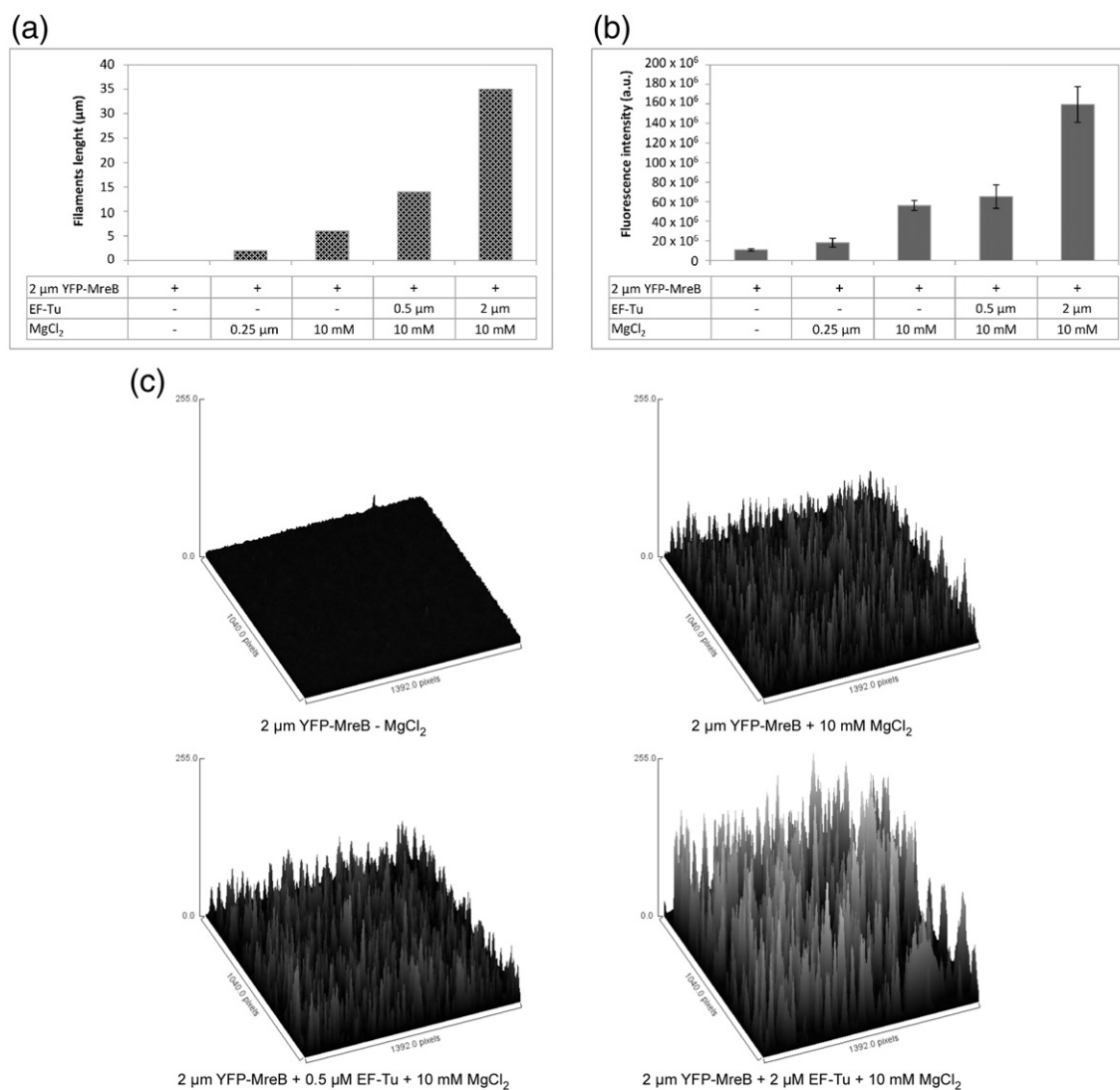


**Fig. 4.** Analysis of fluorescence micrographs of purified YFP-MreB *in vitro* on glass slides. (a) Maximum length of MreB filaments and (b) total fluorescence intensities of micrographs. We analyze 15–20 micrographs for each condition. (c) Surface plot giving three-dimensional graphs of the intensities of pixels in grayscale of typical YFP-MreB micrograph at indicated condition. Analysis were done using ImageJ v1.48 [51].

there is a higher fluctuation of signals in *B. subtilis* cells because the filaments are curved along the membrane, in contrast to the many rather straight filaments in *E. coli* cells. Thus, the turnover of *B. subtilis* MreB filaments is about 2.5-fold higher in *B. subtilis* cells than in *E. coli* cells, at least in part dependent on the fact that MreB filaments are dynamic in *B. subtilis*, but not in *E. coli* cells.

## Discussion

Our work provides several key findings on MreB that are of conceptual importance. Super-resolution experiments have recently shown that, similar to actin

polymers, the basic structures formed by MreB are filaments, which extend mostly for a half-turn around the cell's circumference and sometimes even further in *B. subtilis* and *E. coli* [37,38]. Thus, long polymers formed by MreB *in vivo* can offer structural support for long range and stable interaction between different enzymatic complexes at or in the membrane, including enzymes involved in cell wall synthesis.

We now show that translation elongation factor EF-Tu affects the formation of MreB filaments and thus a modulator of a bacterial actin-like protein. EF-Tu has been shown to interact with MreB *in vivo* and *in vitro* in *E. coli* and *B. subtilis* cells [23,24], and both factors affect each other's localization in *B. subtilis* cells [23]. A partial depletion of EF-Tu

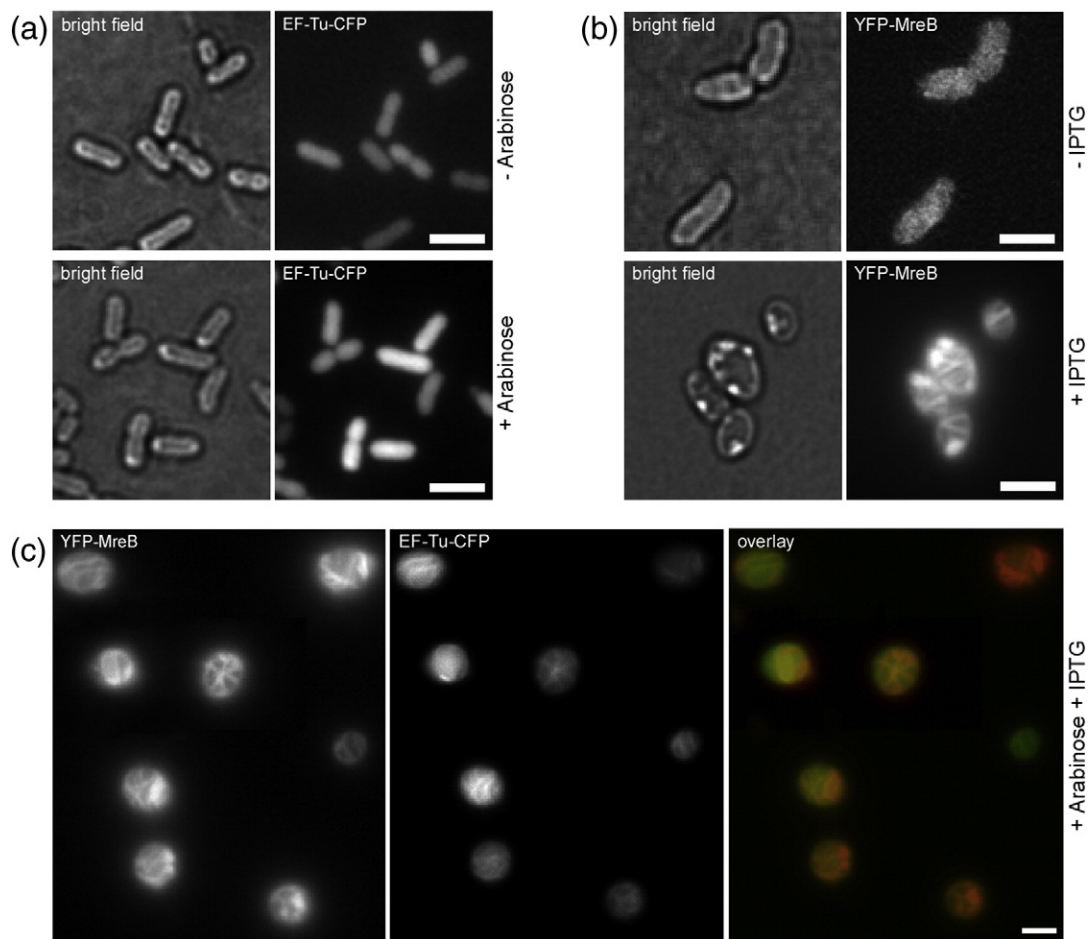


**Fig. 5.** Effect of MreB filaments on EF-Tu *in vivo*. Heterologous expression of proteins in *E. coli* cells, in the absence of inducer (–IPTG for YFP-MreB/–arabinose for EF-Tu-CFP) or 60 min after induction of transcription [+IPTG (0.25 mM)/arabinose (0.02%)]. (a) YFP-MreB, (b) EF-Tu-CFP, (c) expression of both YFP-MreB and EF-Tu-CFP from two compatible pCDF-Duet and pBAD33 plasmids, respectively. Overlay: EF-Tu-CFP, green; YFP-MreB, red. Scale bars represent 2  $\mu$ m.

does not have a strong effect on translation, but it leads to a defect in cell shape, suggesting that EF-Tu has an influence on cell morphology via an interaction with MreB, in addition to its essential function in translation [23]. In this work, we show that EF-Tu affects the formation of MreB filaments *in vitro*, and MreB affects the localization of EF-Tu *in vivo* in a heterologous cell system. In agreement with their specific interaction *in vitro* and in *B. subtilis* [23], we show that EF-Tu and MreB co-localize in *E. coli* cells and that MreB recruits EF-Tu to the filaments, validating the findings from *B. subtilis* cells that both proteins influence each other's subcellular positioning. The most important finding of this study is that purified EF-Tu enhances the ability of MreB to form filaments and increases the rate of filament formation. The effect of EF-Tu on MreB polymer formation was concentration dependent, and EF-Tu co-sedimented with MreB filaments, suggesting that EF-Tu remains bound to MreB filaments as it accelerates filament

assembly, which is also supported by the formation of EF-Tu/MreB filaments in *E. coli* cells.

It is interesting to note that, in our study, MreB filaments formed within few seconds and remained stable for an extended time, revealing that MreB can polymerize much faster than actin *in vitro*. It is tempting to speculate that bacterial actin is more potent in polymerizing than the eukaryotic counterpart, which has evolved to be regulated by a multitude of effectors. How might EF-Tu affect MreB filament formation? Actin filaments show a high degree of structural plasticity, and a change in the arrangement of actin subunits via actin interactors alters filament architecture and dynamics [39]. As EF-Tu and MreB appear to interact at a 1:1 stoichiometry even as monomers, as determined in cross-linking assays, as well as co-sedimentation, EF-Tu may affect MreB filament architecture and thereby accelerate filament formation. EF-Tu could also affect the dynamics of MreB filament formation by affecting ATP hydrolysis of

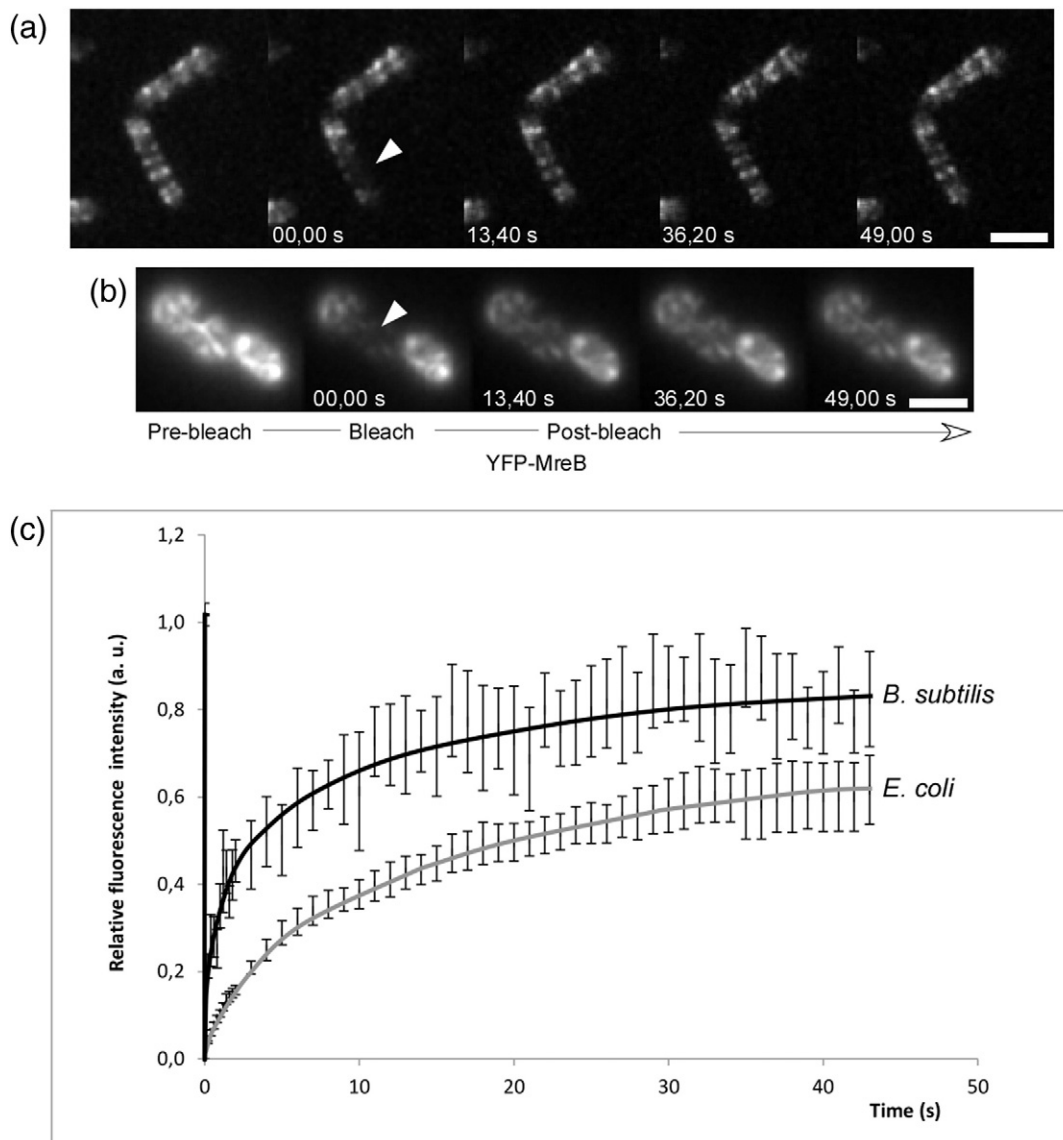


**Fig. 6.** FRAP analysis of YFP-MreB. (a) In *B. subtilis* cells (JS36: *P<sub>xyl</sub>-yfp-mreB spec::amy* [15]); (b) heterologously expressed in *E. coli* cells. White triangle indicates the area of bleaching; numbers indicate time in seconds after bleaching. Scale bars represent 2  $\mu\text{m}$ . (c) Analysis of FRAP experiments from *B. subtilis* cells (black line) or from *E. coli* cells (gray line). Plot of relative fluorescence intensity as a function of time (s), corrected for background brightness and total YFP fading over time period. The prebleach intensity is set at 100%, and the postbleach intensity is set as “0”. The graph represents the average of five and six FRAP experiments from *B. subtilis* and *E. coli*, respectively. Bars represent standard error of the mean.

MreB subunits. It is also possible that EF-Tu increases MreB polymerization via an effect on plasticity. Indeed, MreB has been observed in different conformations within filaments *in vitro* [5,40], indicating a high degree of structural flexibility.

Lowered levels of EF-Tu lead to the formation of fewer aberrantly localized MreB filaments in *B. subtilis* [23]. Our data showing that EF-Tu is recruited to filamentous MreB structures in a heterologous cell system support the model that MreB is able to direct

the localization of EF-Tu *in vivo*. EF-Tu structures underneath the cell membrane are much more static than MreB filaments in *B. subtilis* [23], such that EF-Tu structures could serve as tracks for MreB filaments. In turn, EF-Tu may stimulate the assembly of MreB filaments, which could extend and retract along EF-Tu structures. Interestingly, we show in this work that *B. subtilis* MreB filaments have a higher turnover in *B. subtilis* cells than in *E. coli* cells, as determined using FRAP. Half-time recovery of MreB filaments is

18 s in *B. subtilis* cells and is 50 s when expressed heterologously in *E. coli* cells. However, slower FRAP recovery in *E. coli* cells is at least partially due to the fact that heterologously expressed MreB filaments do not move in a circumferential manner, and thus, the 50-s half-time recovery rate actually reflects the true subunit exchange kinetics within MreB filaments. These experiments reveal that the turnover of MreB filaments is much higher than previously anticipated [15,33] and is also much higher than that of *E. coli* MreB expressed in fission yeast cells [41] but is similar to that of the FtsZ ring structure at mid-cell [35]. Of note, both the movement of complete polymers and the exchange of monomers are the basis for the fast recovery observed for MreB in the cell during FRAP experiments. Our data thus show that MreB filament dynamics are markedly different in different cellular contexts.

Among bacterial cytoskeletal proteins, the regulation of polymer formation for the tubulin-like protein FtsZ that builds up the cytokinetic Z-ring is well understood [42,43]. In contrast, the cellular factors regulating the dynamics of MreB filaments and thus its function are poorly unveiled. Our previous work has revealed an interplay between MreB and EF-Tu [23]. Recently, it was shown that chromosomally encoded toxin-antitoxin systems can inhibit the polymerization or promote the bundling of both MreB and FtsZ in *E. coli* [44–46]. We demonstrate in our present work that the activity of MreB filaments can be modulated by an additional factor in *B. subtilis* and that EF-Tu directly affects filament formation of MreB. Interestingly, the eukaryotic ortholog of EF-Tu, elongation factor EF-1 $\alpha$ , also interacts with actin and influences actin filaments [47–49], apparently through bundling of actin filaments [50]. Thus, the interaction EF-Tu/MreB and EF-1 $\alpha$ /actin is evolutionarily conserved and apparently highly relevant for the physiology of the cell.

## Materials and Methods

### Plasmids construction

pJS63 (*smP<sub>T7lac</sub>-Strep-tag-mreB*) was constructed by amplification of the *Strep-mreB* sequence from *B. subtilis* wild-type (PY79) chromosomal DNA using an upstream primer containing the *Strep-tag* sequence. The resulted PCR product was inserted between NdeI and XhoI restriction sites in pCDFDuet vector (from Novagen). For pJS64 (*smP<sub>T7lac</sub>-Strep-tag-yfp-mreB*), the *Strep-yfp-mreB* sequence was amplified from pJS24 [15] plasmid (*bla amyE::Pxyl-yfp-mreB spec*) using an upstream primer containing *Strep-tag* sequence. The resulted PCR product was inserted between NdeI and XhoI restriction sites in pCDFDuet vector. For pJS65 (*bla P<sub>T7lac</sub>-tufA-Strep-tag*), the *tufA-Strep-tag* sequence was amplified from the chromosomal DNA of *B. subtilis* wild type (PY79) using a downstream primer containing *Strep-tag* sequence. The

resulted PCR product was inserted between NdeI and XhoI restriction sites in pETDuet vector (from Novagen). For pJS66 (*bla P<sub>T7lac</sub>-tufA-Bscfp-Strep*), the *tufA-Bscfp-Strep-tag* sequence was amplified from the JS88 strain (*tufA-Bscfp*) [23] using a downstream primer containing *Strep-tag* sequence. The resulted PCR product was inserted between NdeI and XhoI restriction sites in pETDuet vector. For pJS67 (*bla P<sub>T7lac</sub>-tufA-His-tag*), *tufA-His-tag* sequence was amplified from *B. subtilis* (wild-type) chromosomal DNA using a downstream primer containing *His-tag* sequence. The resulting PCR product was inserted between NdeI and XhoI in pETDuet vector. Low expression of EF-Tu or EF-Tu-BsCFP was achieved using pBAD33 plasmid that bears a tight arabinose promoter. The *tufA* or *tufA-Bscfp* gene was amplified as described above and inserted between KpnI and HindIII in pBAD33 generating pJS80 (*cat P<sub>BAD</sub>-tufA*) and pJS81 (*cat P<sub>BAD</sub>-tufA-Bscfp*), respectively.

### Expression and purification of proteins

*E. coli* BL21( $\lambda$ DE3) cells transformed with pJS63 and pJS67 (for Strep-MreB and EF-Tu-His co-purification strain), pJS63, pJS64 or pJS65 were inoculated in 400 ml of LB supplemented with Streptomycin (50  $\mu$ g/ml) or ampicillin (100  $\mu$ g/ml) and grown at 37 °C until an OD<sub>600</sub> reached 0.6–0.8. The expression of proteins was induced by adding 1 mM IPTG to the culture, which was left to grow for an additional 4 h. Cells were spun down at 6000 rpm at 4 °C for 15 min and the pellet was quickly frozen in liquid nitrogen and stored at –80 °C until use. Cells were disrupted with a French press in appropriate buffers and the lysate was cleared by centrifugation at 16,000 rpm and 4 °C for 30 min. Strep-tagged proteins were purified using Strep-tag purification kit purchased from IBA GmbH. The purified proteins were dialyzed against the polymerization buffer [5 mM Tris–Cl (pH 7.4), 0.1 mM CaCl<sub>2</sub> and 0.2 mM ATP] before storage.

### Cross-linking assay

Cross-linking with glutaraldehyde was carried out in 100 mM phosphate buffer (pH 8.0) at room temperature. Strep-MreB and EF-Tu-His eluted from Streptavidin column were incubated with 0.05% glutaraldehyde for 5, 10 and 15 min, respectively. The reactions were quenched by the addition of 100 mM Tris (pH 7.5), and samples were resolved on 8% SDS-PAGE. BS3 reactions were performed likewise, except that the cross-linking time was prolonged 15, 30 and 45 min, respectively, with 0.5 mM BS3. The experiment was performed in duplicate. One gel was silver stain for direct visualization of the proteins bands and the proteins from the second gel were transferred to nitrocellulose membrane. MreB was detected by Western blotting with anti-MreB antibodies.

### In vitro polymerization assay

For the fluorescence microscopy analysis of YFP-MreB, clarified (centrifugation at 100,000g for 15 min at 4 °C) Strep-YFP-MreB (2  $\mu$ M) was added to the polymerization buffer [5 mM Tris–Cl (pH 7.4), 0.1 mM CaCl<sub>2</sub> and 0.2 mM ATP] and the polymerization was initiated by adding 5 mM MgCl<sub>2</sub>. The mixture was incubated at room temperature for

about 10 min prior to the microscopy. To assess the effect of EF-Tu on the formation of MreB Polymers, we added EF-Tu-Strep to the mixture before incubation.

For sedimentation assays, 10  $\mu$ M or 20  $\mu$ M of clarified Strep-MreB or Strep-YFP-MreB was added to the polymerization buffer and the mixture was incubated at room temperature with or without MgCl<sub>2</sub> (5 mM) for 15 min. For co-sedimentation assay, EF-Tu-Strep was added to the mixture at different ratio relative to Strep-MreB or Strep-YFP-MreB before incubation. Afterwards, protein samples were centrifuged at 100,000g for 20 min at 4 °C. Supernatants and pellets (resuspended in an equal volume as the supernatants) were analyzed by SDS-PAGE and Coomassie blue staining.

### Light-scattering assay

Light scattering was measured at 418 nm after excitation at 315 nm in a Shimadzu RF-5001PC or PerkinElmer LS55 fluorimeter. The scattered light intensity was measured at an angle of 90° from the direction of the incident light. The temperature was set in the cuvette (Quartz SUPRASIL Ultra-micro from PerkinElmer) at 25 °C. Appropriate concentration of proteins samples was added to the polymerization buffer to a final volume of 100  $\mu$ l. The mixture was equilibrated at 25 °C for 2 min before adding magnesium that triggered the polymerization.

### Microscopy and FRAP analysis

Epi-fluorescence microscopy was performed using a Zeiss Axio Imager equipped with a digital charge-coupled device camera and total internal reflection fluorescence objective with an aperture of 1.45. Images were captured using Metamorph 6.3 software. FRAP experiments were performed on a Zeiss Axio Observer using a 405-nm laser focussed to a 1- $\mu$ m beam at the focal plane (Visitron, Munich, Germany). Images were analyzed using Metamorph 6.3 or ImageJ<sup>†</sup> (v1.46r; Rasband WS, ImageJ, US National Institutes of Health, Bethesda, MD, USA, 1997–2012) [51]. For stack alignment of images, the StackReg plugin was used [52]. Gradual bleaching of the image during acquisition was compensated by normalizing the fluorescence of the bleached region to the integral fluorescence of the entire cell in the same image, and background fluorescence was subtracted. The relative fluorescence intensity of the region of interest of the image sequence was normalized to the relative region of interest intensity before bleaching. Time lapse microscopy of *E. coli* cells expressing YFP-BsMreB was acquired by SIM using a Zeiss Elyra system.

### Filament length and fluorescence intensity measurements

Filament length and fluorescence intensities were measured using ImageJ<sup>1</sup> (v1.48; Rasband WS, ImageJ, US National Institutes of Health, Bethesda, MD, USA, 1997–2014) [51]. Before measurements, background in the images was subtracted using the “Subtract Background” tool. The “Rolling Ball Radius” was set to the default value of 50.0 pixels. Filaments length was measured using “Free-hand Line Selection” tool and fluorescence intensity measurements were set to measure the integrated fluores-

cence density of the total area in images. “Surface Plot” tool was used to obtain a three-dimensional graph of the intensities of pixels in a grayscale.

Supplementary data to this article can be found online at <http://dx.doi.org/10.1016/j.jmb.2015.01.025>.

## Acknowledgments

We thank Luise Simon for help with analysis of FRAP data. This work was funded by the priority program SPP1464 of the Deutsche Forschungsgemeinschaft, by FOR 929 and by the LOEWE funding from the state of Hessen.

Received 7 October 2014;

Received in revised form 2 January 2015;

Accepted 27 January 2015

Available online 10 February 2015

### Keywords:

bacterial cytoskeleton;  
translation factor Tu;  
MreB;  
actin

<sup>4</sup>Present address: Division of Infectious Diseases, University Medical Center Freiburg, Hugstetter Strasse 55, 79106 Freiburg, Germany.

<sup>†</sup><http://imagej.nih.gov/ij/>.

### Abbreviations used:

FRAP, fluorescence recovery after photobleaching; SIM, structured illumination microscopy.

## References

- [1] Waterbury JB, Willey JM, Franks DG, Valois FW, Watson SW. A cyanobacterium capable of swimming motility. *Science* 1985; 230:74–6.
- [2] Ursell T, Chau RM, Wisen S, Bhaya D, Huang KC. Motility enhancement through surface modification is sufficient for cyanobacterial community organization during phototaxis. *PLoS Comput Biol* 2013;9:e1003205.
- [3] El-Sharoud WM, Graumann PL. Cold shock proteins aid coupling of transcription and translation in bacteria. *Sci Prog* 2007;90:15–27.
- [4] Carballido-Lopez R. The bacterial actin-like cytoskeleton. *Microbiol Mol Biol Rev* 2006;70:888–909.
- [5] van den Ent F, Amos LA, Lowe J. Prokaryotic origin of the actin cytoskeleton. *Nature* 2001;413:39–44.
- [6] Mayer JA, Amann KJ. Assembly properties of the *Bacillus subtilis* actin, MreB. *Cell Motil Cytoskeleton* 2009;66: 109–18.
- [7] Popp D, Narita A, Maeda K, Fujisawa T, Ghoshdastider U, Iwasa M, et al. Filament structure, organization, and dynamics in MreB sheets. *J Biol Chem* 2010;285:15858–65.

- [8] Bremer A, Millonig RC, Sutterlin R, Engel A, Pollard TD, Aebi U. The structural basis for the intrinsic disorder of the actin filament: the "lateral slipping" model. *J Cell Biol* 1991;115:689–703.
- [9] Jones LJ, Carballido-Lopez R, Errington J. Control of cell shape in bacteria: helical, actin-like filaments in *Bacillus subtilis*. *Cell* 2001;104:913–22.
- [10] Kruse T, Moller-Jensen J, Lobner-Olesen A, Gerdes K. Dysfunctional MreB inhibits chromosome segregation in *Escherichia coli*. *EMBO J* 2003;22:5283–92.
- [11] Figge RM, Divakaruni AV, Gober JW. MreB, the cell shape-determining bacterial actin homologue, co-ordinates cell wall morphogenesis in *Caulobacter crescentus*. *Mol Microbiol* 2004;51:1321–32.
- [12] Waidner B, Specht M, Dempwolff F, Haeberer K, Schaetzle S, Speth V, et al. A novel system of cytoskeletal elements in the human pathogen *Helicobacter pylori*. *PLoS Pathog* 2009;5:e1000669.
- [13] Dye NA, Pincus Z, Theriot JA, Shapiro L, Gitai Z. Two independent spiral structures control cell shape in *Caulobacter*. *Proc Natl Acad Sci USA* 2005;102:18608–13.
- [14] Kruse T, Bork-Jensen J, Gerdes K. The morphogenetic MreBCD proteins of *Escherichia coli* form an essential membrane-bound complex. *Mol Microbiol* 2005;55:78–89.
- [15] Defeu Soufo HJ, Graumann PL. Dynamic localization and interaction with other *Bacillus subtilis* actin-like proteins are important for the function of MreB. *Mol Microbiol* 2006;62:1340–56.
- [16] Kawai Y, Daniel RA, Errington J. Regulation of cell wall morphogenesis in *Bacillus subtilis* by recruitment of PBP1 to the MreB helix. *Mol Microbiol* 2009;71:1131–44.
- [17] Dempwolff F, Reimold C, Reth M, Graumann PL. *Bacillus subtilis* MreB orthologs self-organize into filamentous structures underneath the cell membrane in a heterologous cell system. *PLoS One* 2011;6:e27035.
- [18] Salje J, van den Ent F, de Boer P, Lowe J. Direct membrane binding by bacterial actin MreB. *Mol Cell* 2011;43:478–87.
- [19] Divakaruni AV, Loo RR, Xie Y, Loo JA, Gober JW. The cell-shape protein MreC interacts with extracytoplasmic proteins including cell wall assembly complexes in *Caulobacter crescentus*. *Proc Natl Acad Sci USA* 2005;102:18602–7.
- [20] Daniel RA, Errington J. Control of cell morphogenesis in bacteria: two distinct ways to make a rod-shaped cell. *Cell* 2003;113:767–76.
- [21] Kim SY, Gitai Z, Kinkhabwala A, Shapiro L, Moerner WE. Single molecules of the bacterial actin MreB undergo directed treadmilling motion in *Caulobacter crescentus*. *Proc Natl Acad Sci USA* 2006;103:10929–34.
- [22] Defeu Soufo HJ, Graumann PL. Dynamic movement of actin-like proteins within bacterial cells. *EMBO Rep* 2004;5:789–94.
- [23] Defeu Soufo HJ, Reimold C, Linne U, Knust T, Gescher J, Graumann PL. Bacterial translation elongation factor EF-Tu interacts and colocalizes with actin-like MreB protein. *Proc Natl Acad Sci USA* 2010;107:3163–8.
- [24] Liu Z, Xing D, Su QP, Zhu Y, Zhang J, Kong X, et al. Super-resolution imaging and tracking of protein-protein interactions in sub-diffraction cellular space. *Nat Commun* 2014;5:4443.
- [25] Mayer F. Cytoskeletal elements in bacteria *Mycoplasma pneumoniae*, *Thermoanaerobacterium* sp., and *Escherichia coli* as revealed by electron microscopy. *J Mol Microbiol Biotechnol* 2006;11:228–43.
- [26] Rial DV, Ceccarelli EA. Removal of DnaK contamination during fusion protein purifications. *Protein Expr Purif* 2002;25:503–7.
- [27] Pollard TD. Measurement of rate constants for actin filament elongation in solution. *Anal Biochem* 1983;134:406–12.
- [28] Pollard TD. Assembly and dynamics of the actin filament system in nonmuscle cells. *J Cell Biochem* 1986;31:87–95.
- [29] Defeu Soufo HJ, Graumann PL. *Bacillus subtilis* MreB paralogues have different filament architectures and lead to shape remodelling of a heterologous cell system. *Mol Microbiol* 2010;78:1145–58.
- [30] Azam TA, Hiraga S, Ishihama A. Two types of localization of the DNA-binding proteins within the *Escherichia coli* nucleoid. *Genes Cells* 2000;5:613–26.
- [31] Lewis PJ, Thaker SD, Errington J. Compartmentalization of transcription and translation in *Bacillus subtilis*. *EMBO J* 2000;19:710–8.
- [32] Mascarenhas J, Weber MH, Graumann PL. Specific polar localization of ribosomes in *Bacillus subtilis* depends on active transcription. *EMBO Rep* 2001;2:685–9.
- [33] Carballido-Lopez R, Errington J. The bacterial cytoskeleton: *in vivo* dynamics of the actin-like protein Mbl of *Bacillus subtilis*. *Dev Cell* 2003;4:19–28.
- [34] Kumar M, Mommer MS, Sourjik V. Mobility of cytoplasmic, membrane, and DNA-binding proteins in *Escherichia coli*. *Biophys J* 2010;98:552–9.
- [35] Anderson DE, Gueiros-Filho FJ, Erickson HP. Assembly dynamics of FtsZ rings in *Bacillus subtilis* and *Escherichia coli* and effects of FtsZ-regulating proteins. *J Bacteriol* 2004;186:5775–81.
- [36] Hu Z, Gogol EP, Lutkenhaus J. Dynamic assembly of MinD on phospholipid vesicles regulated by ATP and MinE. *Proc Natl Acad Sci USA* 2002;99:6761–6.
- [37] Reimold C, Defeu Soufo HJ, Dempwolff F, Graumann PL. Motion of variable-length MreB filaments at the bacterial cell membrane influences cell morphology. *Mol Biol Cell* 2013;24:2340–9.
- [38] Olshausen PV, Defeu Soufo HJ, Wicker K, Heintzmann R, Graumann PL, Rohrbach A. Superresolution imaging of dynamic MreB filaments in *B. subtilis*—a multiple-motor-driven transport? *Biophys J* 2013;105:1171–81.
- [39] Kueh HY, Mitchison TJ. Structural plasticity in actin and tubulin polymer dynamics. *Science* 2009;325:960–3.
- [40] Shiomi D, Niki H. A mutation in the promoter region of zipA, a component of the divisome, suppresses the shape defect of RodZ-deficient cells. *MicrobiologyOpen* 2013;2:798–810.
- [41] Srinivasan R, Mishra M, Murata-Hori M, Balasubramanian MK. Filament formation of the *Escherichia coli* actin-related protein, MreB, in fission yeast. *Curr Biol* 2007;17:266–72.
- [42] Romberg L, Levin PA. Assembly dynamics of the bacterial cell division protein FtsZ : poised at the edge of stability. *Annu Rev Microbiol* 2003;57:125–54.
- [43] Margolin W. FtsZ and the division of prokaryotic cells and organelles. *Nat Rev Mol Cell Biol* 2005;6:862–71.
- [44] Tan Q, Awano N, Inouye M. YeeV is an *Escherichia coli* toxin that inhibits cell division by targeting the cytoskeleton proteins, FtsZ and MreB. *Mol Microbiol* 2011;79:109–18.
- [45] Masuda H, Tan Q, Awano N, Yamaguchi Y, Inouye M. A novel membrane-bound toxin for cell division, CptA (YgfX), inhibits polymerization of cytoskeleton proteins, FtsZ and MreB, in *Escherichia coli*. *FEMS Microbiol Lett* 2012;328:174–81.
- [46] Masuda H, Tan Q, Awano N, Wu KP, Inouye M. YeeU enhances the bundling of cytoskeletal polymers of MreB and FtsZ, antagonizing the CbtA (YeeV) toxicity in *Escherichia coli*. *Mol Microbiol* 2012;84:979–89.
- [47] Gross SR, Kinzy TG. Translation elongation factor 1A is essential for regulation of the actin cytoskeleton and cell morphology. *Nat Struct Mol Biol* 2005;12:772–8.

- 
- [48] Liu G, Tang J, Edmonds BT, Murray J, Levin S, Condeelis J. F-actin sequesters elongation factor 1alpha from interaction with aminoacyl-tRNA in a pH-dependent reaction. *J Cell Biol* 1996;135:953–63.
- [49] Liu G, Grant WM, Persky D, Latham VM, Singer RH, Condeelis J. Interactions of elongation factor 1alpha with F-actin and beta-actin mRNA: implications for anchoring mRNA in cell protrusions. *Mol Biol Cell* 2002;13:579–92.
- [50] Yang F, Demma M, Warren V, Dharmawardhane S, Condeelis J. Identification of an actin-binding protein from *Dictyostelium* as elongation factor 1a. *Nature* 1990;347:494–6.
- [51] Schneider CA, Rasband WS, Eliceiri KW. NIH Image to ImageJ: 25 years of image analysis. *Nat Methods* 2012;9:671–5.
- [52] Thevenaz P, Ruttimann UE, Unser M. A pyramid approach to subpixel registration based on intensity. *IEEE Trans Image Process* 1998;7:27–41.